



# Pre-equilibrium dynamics and heavy-ion observables<sup>☆</sup>

Ulrich Heinz and Jia Liu

*Physics Department, The Ohio State University, Columbus, OH 43210, USA*

---

## Abstract

To bracket the importance of the pre-equilibrium stage on relativistic heavy-ion collision observables, we compare simulations where it is modeled by either free-streaming partons or fluid dynamics. These cases implement the assumptions of extremely weak vs. extremely strong coupling in the initial collision stage. Accounting for flow generated in the pre-equilibrium stage, we study the sensitivity of radial, elliptic and triangular flow on the switching time when the hydrodynamic description becomes valid. Using the hybrid code iEBE-VISHNU [1] we perform a multi-parameter search, constrained by particle ratios, integrated elliptic and triangular charged hadron flow, the mean transverse momenta of pions, kaons and protons, and the second moment  $\langle p_T^2 \rangle$  of the proton transverse momentum spectrum, to identify optimized values for the switching time  $\tau_s$  from pre-equilibrium to hydrodynamics, the specific shear viscosity  $\eta/s$ , the normalization factor of the temperature-dependent specific bulk viscosity  $(\zeta/s)(T)$ , and the switching temperature  $T_{sw}$  from viscous hydrodynamics to the hadron cascade UrQMD. With the optimized parameters, we predict and compare with experiment the  $p_T$ -distributions of  $\pi$ ,  $K$ ,  $p$ ,  $\Lambda$ ,  $\Xi$  and  $\Omega$  yields and their elliptic flow coefficients, focusing specifically on the mass-ordering of the elliptic flow for protons and Lambda hyperons which is incorrectly described by VISHNU without pre-equilibrium flow.

**Keywords:** collective flow, pre-equilibrium dynamics, quark-gluon plasma, viscosity, model-to-data comparison, parameter optimization, uncertainty quantification

---

## 1. Introduction

Relativistic viscous hydrodynamics has become the workhorse of dynamical modeling of ultra-relativistic heavy-ion collisions. However, hydrodynamics does not become valid until the medium has reached a certain degree of local momentum isotropization [2]. In an inhomogeneous system, collective flow (i.e. space-momentum correlations) begins, however, to develop already before hydrodynamics becomes valid. The hydrodynamic stage thus starts with a non-vanishing pre-equilibrium flow [3–7]. In [8] we therefore performed a systematic study of pre-equilibrium flow effects on heavy-ion collision observables. We here summarize the main results of this study and add a few recent results that go beyond the work reported in [8].

---

<sup>☆</sup>Work supported by the DOE, Office of Science, Office of Nuclear Physics under Award No. DE-SC0004286. Computing resources provided by the [Ohio Supercomputer Center](#). Thanks to Chun Shen for fruitful discussions.

## 2. The model

We assume longitudinal boost-invariance and model the approach towards local thermal equilibrium in a heavy-ion collision very simply [8] as a pre-equilibrium stage of noninteracting free-streaming massless partonic degrees of freedom, separated by a switching time  $\tau_s$  from a strongly coupled quark-gluon plasma (QGP) stage in which frequent collisions isotropize the local momentum distribution sufficiently quickly that it can be described by viscous relativistic fluid dynamics. The variable switching time  $\tau_s$  parametrizes the duration of the thermalization process. For massless degrees of freedom the evolution of the energy-momentum tensor during the free-streaming stage is independent of the initial transverse momentum distribution as long as it starts out locally azimuthally symmetric, and can be solved analytically [8].

At  $\tau_s$  we Landau-match the analytically evolved pre-equilibrium energy-momentum tensor to viscous hydrodynamic form [8]. Space-momentum correlations established by the free-streaming dynamics in the pre-equilibrium stage manifest themselves as non-zero initial values for the hydrodynamic flow velocity profiles, giving rise to non-zero initial radial and anisotropic flows. Local momentum anisotropies resulting from the free-streaming evolution of a spatially inhomogeneous initial density profile generate nonzero initial values for the shear stress. Matching the traceless pre-equilibrium energy-momentum tensor of noninteracting massless degrees of freedom to a non-conformal, lattice QCD based equation of state [9] at  $\tau_s$  generates a non-zero initial bulk viscous pressure field in the hydrodynamic fluid. All of these initial fields are then further evolved with the second-order viscous relativistic fluid dynamics code VISH2+1.

After hadronization of the QGP at a pseudocritical temperature  $T_c \simeq 155$  MeV (determined by the equation of state [9]), the medium constituents are color neutral hadrons whose interactions are weaker than the gluon-mediated interactions in the earlier color-deconfined QGP, causing a rapid growth of their mean free paths and a subsequent breakdown of the fluid dynamic framework. We therefore switch from VISH2+1 to a microscopic description, using the hadron cascade code UrQMD, on an isothermal switching surface of temperature  $T_{sw}$  which we here consider as an unknown parameter to be optimized by comparison with experimental data.

Two additional important parameters affecting the evolution of collective flow and the  $p_T$  distributions of the finally emitted hadrons are the shear and bulk viscosities during the liquid QGP stage. For simplicity, we assume the QGP specific shear viscosity  $\eta/s$  to be a temperature-independent, adjustable constant. For the specific bulk viscosity  $\zeta/s$ , which is expected to develop a strong peak due to critical scattering close to the quark-hadron phase transition, we adopt the temperature-dependent parametrization given in [10] (which features a peak at  $T_{\text{peak}} = 180$  MeV), but consider its normalization as a freely tunable parameter. In practice, peak values of  $\zeta/s$  exceeding 1 (corresponding to bulk viscosity normalization factors  $> 3$ ) cause the (negative) bulk viscous pressure to become very large near  $T_{\text{peak}}$ , leading to negative total pressures and mechanical instability of the medium against cavitation. These physical instabilities also eventually render the hydrodynamic code numerically unstable.

## 3. Results

We found in [8] that an extended pre-equilibrium stage increases the final radial flow, leading to flatter  $p_T$ -spectra, while leaving the integrated charged hadron  $v_2$  and  $v_3$  almost unchanged unless  $\tau_s$  significantly exceeds 2 fm/c. Bulk viscosity inhibits radial flow build-up, so the constraint from the measured  $p_T$  distributions causes a strong positive correlation between  $\tau_s$  and the bulk viscosity normalization factor. The experimental charged hadron elliptic flow constraint anticorrelates bulk and shear viscosity; at low  $p_T$ , the bulk viscous correction  $\delta f_{\text{bulk}}$  at  $T_{sw}$  acts

as an effective positive chemical potential for massive hadrons [12], causing an anticorrelation between the bulk viscosity normalization factor and the chemical decoupling temperature  $T_{sw}$ .

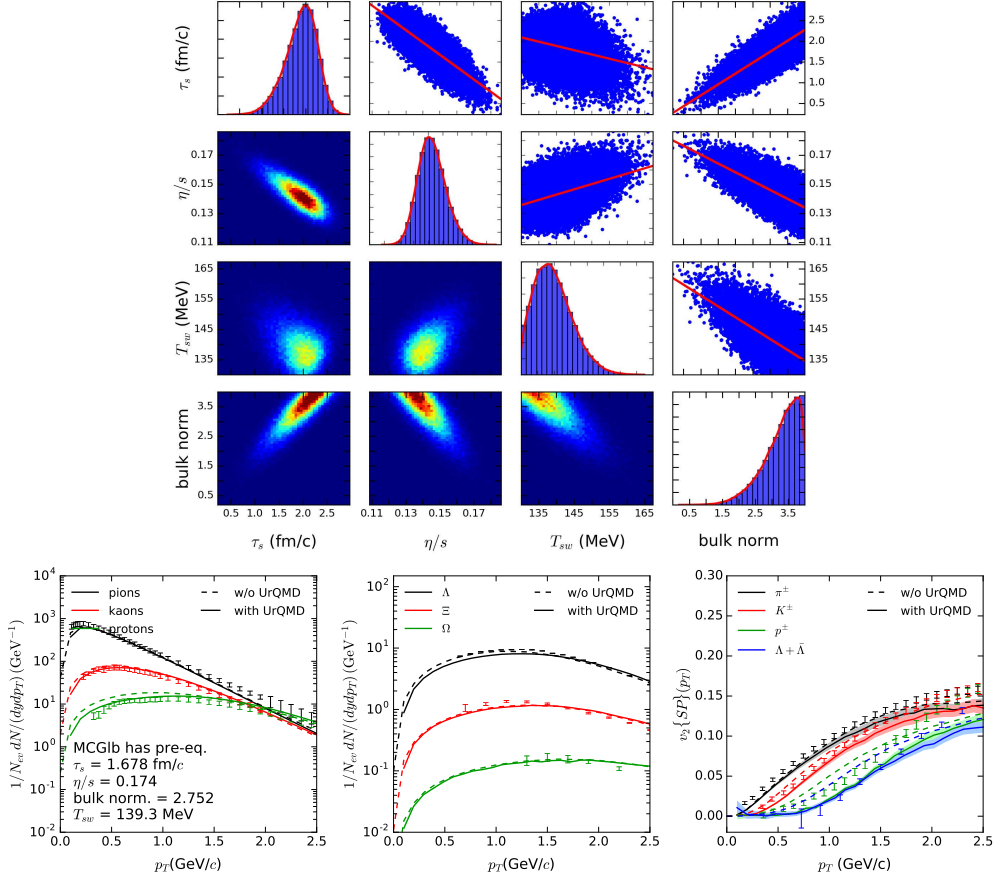


Fig. 1. *Upper panel:* Likelihood distributions for each of the four fit parameters are shown on the diagonal, correlations between them in upper right triangle of plots, and 2-dimensional projections of the likelihood distributions for pairs of parameters (with dark red indicating the most likely regions) in the lower triangle of plots. *Lower panels:*  $p_T$  distributions for pions, kaons and protons (left),  $\Lambda$ ,  $\Xi$  and  $\Omega$  (middle), and the differential elliptic flows for  $\pi$ ,  $K$ ,  $p$  and  $\Lambda$  (right) from 400 hydrodynamic simulations with fluctuating initial conditions, each oversampled 400 times with UrQMD to obtain sufficient particle statistics. Solid lines: full VISHNU runs. Dashed lines: pure hydro runs with immediate freeze-out at  $T_{sw}$ , without subsequent hadronic rescattering using UrQMD. Experimental data from ALICE [11].

These tendencies are illustrated in the top panel of Fig. 1 for which we ran VISHNU simulations with smooth ensemble-averaged MC-Glauber initial conditions for 10-20% central Pb-Pb collisions at 2.76 A GeV for 1000 different quadruplets of the parameters listed in Table 1, calculated the experimental observables listed in the same table (chosen for their insensitivity to initial-state event-by-event fluctuations), determined the  $\chi^2$  for each quadruplet by comparing them with the experimental values, and then reconstructed the posterior likelihood distributions in the 4-dimensional parameter space using MCMC sampling [13]. For the set with the lowest  $\chi^2$ , listed in the lower left panel of Fig. 1, we then ran 400 event-by-event VISHNU simulations with fluctuating initial conditions, each oversampled 400 times in the UrQMD stage for suffi-

cient particle statistics, to predict the full transverse momentum distributions and their elliptic flows  $v_2(p_T)$  for the specific hadron species shown in the bottom row of Fig. 1.

$\langle v_2^{\text{ch}} \rangle$ [14]	$0.0782 \pm 0.0019$	parameter	best	mean	95% C.I.
$\langle v_3^{\text{ch}} \rangle$ [14]	$0.0316 \pm 0.0008$	$\tau_s$ (fm/c)	2.233	1.889	1.187 - 2.591
$\langle p_T \rangle_{\pi^+}$ (GeV/c) [15]	$0.542 \pm 0.018$	$\eta/s$	0.135	0.143	0.124 - 0.161
$\langle p_T \rangle_{K^+}$ (GeV/c) [15]	$0.825 \pm 0.028$	$T_{\text{sw}}$ (MeV)	133.4	134.0	128.5 - 151.1
$\langle p_T \rangle_p$ (GeV/c) [15]	$1.311 \pm 0.043$	bulk norm.	3.998	3.277	N/A
$\langle p_T^2 \rangle_p$ (GeV <sup>2</sup> /c <sup>2</sup> ) [15]	$2.085 \pm 0.070$				
$(dN_{\pi^+}/dy)/(dN_{K^+}/dy)$ [15]	$6.691 \pm 0.670$				
$(dN_{\pi^+}/dy)/(dN_p/dy)$ [15]	$21.667 \pm 2.292$				
$(dN_{\pi^+}/dy)/(dN_{\Lambda}/dy)$ [15]	$26.765 \pm 3.639$				

Table 1. *Left:* Measured values of nine hadronic observables from 2.76 A TeV 10–20% central Pb+Pb collisions used to constrain the model parameters listed on the right.  $\langle p_T \rangle$  and  $\langle p_T^2 \rangle$  are truncated means calculated from the data tables for the transverse momentum distributions listed in [15]. *Right:* Best-fit parameters and 95% confidence intervals (C.I.) using the results from Markoff Chain Monte Carlo sampling of the posterior parameter distribution shown in Fig. 1 (top).

To illustrate the effect of the microscopically simulated late hadronic rescattering stage on these observables we also added dashed lines illustrating their state at the end of the fluid stage at  $T_{\text{sw}}$ . Protons and  $\Lambda$ s experience a significant radial boost from UrQMD, pushing their yields and elliptic flows to larger transverse momenta. Since  $\Lambda$ s in UrQMD scatter with reduced cross sections relative to those of protons, this shift towards larger  $p_T$  is weaker for  $\Lambda$ s than for protons; as a result, the hydrodynamically predicted elliptic flow mass ordering between protons and  $\Lambda$ s at  $T_{\text{sw}}$ , clearly visible in the dashed lines in the lower right panel of Fig. 1 and also in the experimental data [11], is basically eliminated after hadronic rescattering, although not inverted as previously observed in the VISHNU model without pre-equilibrium dynamics [16]. A shorter lifetime of the hadronic rescattering stage could help to keep this from happening.

## References

- [1] C. Shen, Z. Qiu, H. Song, J. Bernhard, S. Bass and U. Heinz, Comput. Phys. Commun. **199** (2016) 61.
- [2] U. Heinz et al., Nucl. Phys. A, in press [arXiv:1509.05818 [nucl-th]].
- [3] P. F. Kolb and R. Rapp, Phys. Rev. C **67** (2003) 044903; P. F. Kolb, [PhD thesis](#), Universität Regensburg, 2002.
- [4] W. Broniowski, W. Florkowski, M. Chojnacki and A. Kisiel, Phys. Rev. C **80** (2009) 034902.
- [5] B. Schenke, P. Tribedy and R. Venugopalan, Phys. Rev. Lett. **108** (2012) 252301.
- [6] W. van der Schee, P. Romatschke and S. Pratt, Phys. Rev. Lett. **111** (2013) 222302.
- [7] P. Romatschke, Eur. Phys. J. C **75** (2015) 429.
- [8] J. Liu, C. Shen and U. Heinz, Phys. Rev. C **91** (2015) 064906.
- [9] A. Bazavov et al. [HotQCD Collaboration], Phys. Rev. D **90** (2014) 094503.
- [10] G. S. Denicol, T. Kodama, T. Koide and P. Mota, Phys. Rev. C **80** (2009) 064901.
- [11] R. Preghenella [ALICE Collaboration], arXiv:1203.5904 [hep-ex]; B. B. Abelev et al. [ALICE Collaboration], JHEP **1506** (2015) 190; Phys. Rev. Lett. **111** (2013) 222301; Phys. Lett. B **728** (2014) 216.
- [12] K. Dusling and T. Schäfer, Phys. Rev. C **85** (2012) 044909.
- [13] C. Quammen, H. Canary, R. M. Taylor II, S. Pratt and J. Wyka <https://github.com/MADAI/DistributionSampling/blob/master/doc/manual/>
- [14] G. Aad et al. [ATLAS Collaboration], JHEP **1311** (2013) 183.
- [15] B. B. Abelev et al. [ALICE Collaboration], Phys. Rev. C **88** (2013) 044910; Phys. Rev. Lett. **111** (2013) 222301.
- [16] X. Zhu, F. Meng, H. Song and Y. X. Liu, Phys. Rev. C **91** (2015) 034904.